Computational Materials Science 95 (2014) 637–650

Contents lists available at ScienceDirect

Computational Materials Science

journal homepage: www.elsevier.com/locate/commatsci

Elastic moduli of covalently functionalized single layer graphene sheets

P.H. Shah, R.C. Batra *

Department of Biomedical Engineering and Mechanics, Virginia Polytechnic Institute and State University, M/C 0219, Blacksburg, VA 24061, USA

ARTICLE INFO

Article history:
Received 17 March 2014
Received in revised form 10 July 2014
Accepted 29 July 2014

Keywords:
Single layer graphene sheet
Young's modulus
Shear modulus
Covalent functionalization
Molecular mechanics

ABSTRACT

Due to their flexibility, large surface area and high specific mechanical properties, single layer graphene sheets (SLGSs) are potential candidates as filler materials for improving mechanical properties of polymers. Their effective utilization as reinforcements requires strong interfacial binding with the matrix surrounding them. The covalent functionalization of SLGSs is an effective technique to enhance this binding. However, covalent bonds introduced by a functional group usually alter the pristine structure of the SLGS that may affect its mechanical properties. Thus it is important to delineate effects of covalent functionalization on elastic moduli of an SLGS. We consider five groups of different polarities, namely, hydrogen (—H), hydroxyl (—OH), carboxyl (—COOH), amine (—NH_2), and fluorine (—F) as model functional groups and investigate their effects on values of Young's modulus and the shear modulus of the SLGS. We use molecular mechanics (MM) simulations with the MM3 potential and the software TINKER to conduct the study. The pristine and the functionalized SLGSs are deformed in simple tension and simple shear, and from curves of the strain energy density of deformation vs. the axial strain and the shear strain, values of Young's modulus and the shear modulus, respectively, are derived. These values are based on the hypothesis that the response of an SLGS is the same as that of an energetically and geometrically equivalent continuum structure of wall thickness 3.4 Å. It is found that functionalization reduces the elastic moduli of the SLGSs which could be due to nearly 120% local strains induced at the functionalized sites of relaxed but unloaded SLGS, and the change in hybridization from sp^2 to sp^3. The decrease in the value of the modulus increases with an increase in the amount of functionalization but is essentially independent of the functionalizing agent. For 10% functionalization, Young's modulus and the shear modulus of the SLGS are found to decrease by about 73% and 42%, respectively. However, the moduli of a fully functionalized SLGS are about the same as those of a 4% functionalized sheet. Even though the moduli of the pristine armchair and zigzag SLGSs are the same, the moduli of functionalized armchair SLGSs are about 20% less than those of the corresponding zigzag SLGSs. The work will help material scientists interested in designing graphene sheet reinforced polymeric composites.

1. Introduction

A great deal of research has been devoted to investigating mechanical properties of a single layer graphene sheet (SLGS) in the last two decades. Methods used to find values of elastic moduli include ab initio calculations, density functional theory (DFT), molecular mechanics (MM) and molecular dynamics (MD) simulations, continuum theories, and experimental techniques. Many of these approaches hypothesize that the response of an SLGS to an applied load is the same as that of an energetically and geometrically equivalent continuum structure (ECS). Since an SLGS is only an atom thick, it is a challenging task to find the wall thickness of the ECS. In Table 1 we have summarized values of Young's modulus, E, basal plane stiffness, K, Poisson's ratio, ν, and wall thickness, t, obtained by various investigators using different techniques. Here, K, E and t are related by $K = Et$. We note that of the results reported in Table 1, Kudin et al. [3] and Gupta and Batra [12] have found values of the wall thickness to be 0.893 and 1 Å, respectively. Neek-Amal and Peeters [13] assumed it to be 1 Å and other researchers have taken it to equal 3.4 Å, which is the interlayer separation distance in bulk graphite.

Due to their high elastic moduli and large surface area (theoretical limit = 2630 m^2/g) [16], SLGSs are desirable reinforcing materials for improving mechanical properties of polymer based composites. However, in order to effectively utilize SLGSs as reinforcements, it is necessary to achieve their strong interfacial binding with the surrounding matrix. Chemical functionalization involving covalent bonding of functional groups to carbon atoms of the SLGS is an effective method to enhance this binding.

---

* Corresponding author. Tel.: +1 540 231 6051.
E-mail address: rbatra@vt.edu (R.C. Batra).

http://dx.doi.org/10.1016/j.commatsci.2014.07.050
0927-0256/

Table 1
Values of E, K, ν and t for an SLGS reported in the literature.

Author(s)	Method/potential	K (N/m)	E (TPa)	ν	t (Å)
van Lier et al. [1]	Ab initio	~377	1.1		3.4
Liu et al. [2]	Ab initio	~357	1.05	0.186	3.4
Kudin et al. [3]	Ab initio	345	3.86	0.149	0.894
Arroyo and Belytschko [4]	Brenner's 1st generation	236		0.412	
	Brenner's 2nd generation	243		0.397	
Konstantinova et al. [5]	DFT	~420	1.24		3.4
Faccio et al. [6]	DFT	323		0.18	
Klintenberg et al. [7]	DFT	358			
Lee et al. [8]	Nano-indentation (experimental)	340 ± 50			
Reddy et al. [9]	Tersoff–Brenner				
	-Along zigzag	~227	0.669	0.416	3.4
	-Along armchair	~276	0.812	0.465	3.4
Cadelano et al. [10]	Tight binding atomistic simulations	312		0.31	
Jiang et al. [11]	MD with Brenner's 2nd generation potential	318–369	0.95–1.1	0.17	3.35
Gupta and Batra [12]	MM with MM3 potential	340	3.4	0.21	1
Neek-Amal and Peeters [13]	MD with Brenner's bond-order potential		1.3 ± 0.07		1
Neek-Amal and Peeters [14]	MD with Brenner's bond-order potential	164–211	0.49–0.63		3.35
Lajevardipour et al. [15]	Monte Carlo with the valence force field model of Perebeinos and Tersoff	350.42 ± 3.15			

However, the introduction of covalent bonds by functional groups alters the pristine structure of the SLGS that may degrade its mechanical properties. Hence, it is important to determine the effect of covalent functionalization on elastic moduli of SLGSs.

Pei et al. [17,18] investigated mechanical properties of hydrogen (—H) and methyl (—CH_3) functionalized SLGSs using MD simulations with the adaptive intermolecular reactive bond order (AIREBO) potential. They found that Young's modulus of the SLGS decreased by 30% and the tensile strength and the fracture strain dropped by 65% when all atoms of the SLGS were functionalized with hydrogen. For 30% atoms of the SLGS functionalized with the methyl group, the elastic modulus, the tensile strength and the fracture strain were found to decrease by 18%, 43% and 47%, respectively. Zheng et al. [19] used MM and MD simulations and the condensed phase optimized molecular potential for atomistic simulation studies (COMPASS) force field to investigate the effect of chemical functionalization on mechanical properties of an SLGS at 1 K. They found 42.2% reduction in Young's modulus with 16% functionalization with the carboxyl (—COOH) group, and ~41.5% drop in the shear modulus with 7.5% functionalization with the hydroxyl group. Kheirkhah et al. [20] used MD simulations with the AIREBO potential to study shear deformations of —H functionalized SLGSs at 300 K, and found that the shear modulus of the SLGS gradually decreased with an increase in the functionalization to 50% with hydrogen.

The polarity of a functional group covalently bonded to carbon atoms of the SLGS is an important factor in determining binding between the two, and with a matrix material. Here we consider five groups of different polarities, namely, hydrogen (—H), hydroxyl (—OH), carboxyl (—COOH), amine (—NH_2), and fluorine (—F) as model functional groups and determine their effects on elastic moduli of SLGSs for varying percentage of functionalization. We employ MM simulations with the MM3 potential and the freely available software TINKER [21] to perform the study.

2. Molecular mechanics simulations

2.1. Force-field

As in our previous work on single wall carbon nanotubes (SWCNTs) [22] and on SLGSs by Gupta and Batra [12], we use the MM3 potential [23] with higher order expansions and cross-terms to model interatomic interactions. We note that the basal plane stiffness of 340 N/m found using the MM3 potential agrees with that found experimentally [24]. This potential, given by Eq. (1), is suitable for studying deformations of an SLGS because of similarities between sp^2 bonds in the hexagonal structure of graphene and the hexagonal structure of aromatic proteins for which the potential was originally developed. For this potential the energy of the system equals the sum of energies due to bonded and non-bonded interactions. The contributions for bonded interactions come from bond stretching (U_s), in-plane angle bending (U_θ), out-of-plane bending (U_γ), torsion (U_ϕ), and cross-interactions including stretch–bend ($U_{s\theta}$), angle–angle ($U_{\theta\theta'}$) and stretch–torsion ($U_{s\phi}$). The non-bonded interactions are van der Waals (U_{vdW}) and dipole–dipole electrostatic ($U_{\mu\mu'}$).

$$
\begin{aligned}
U_s &= 71.94K_s(r-r_0)^2\left[1-2.55(r-r_0)+\frac{7}{12}(2.55(r-r_0)^2)\right]\\
U_\theta &= 0.0219K_\theta(\theta-\theta_0)^2\bigl[1-0.014(\theta-\theta_0)+5.6(10^{-5})(\theta-\theta_0)^2\\
&\quad -7.0(10^{-7})(\theta-\theta_0)^3+2.2(10^{-8})(\theta-\theta_0)^4\\
U_\gamma &= 0.0219K_\gamma\gamma^2\bigl[1-0.014\gamma+5.6(10^{-5})\gamma^2-7.0(10^{-7})\gamma^3\\
&\quad +2.2(10^{-8})\gamma^4\\
U_\phi &= (V_1/2)(1+\cos\phi)+(V_2/2)(1-\cos 2\phi)+(V_3/2)(1+\cos 3\phi)\\
U_{s\theta} &= 2.511K_{s\theta}\left[(r-r_0)+(r'-r'_0)\right](\theta-\theta_0)\\
U_{\theta\theta'} &= -0.021914K_{\theta\theta'}(\theta-\theta_0)(\theta'-\theta'_0)\\
U_{s\phi} &= -5.9975K_{s\phi}(r-r_0)(1+\cos 3\phi)\\
U_{vdW} &= \varepsilon\left[-2.25(r_v/r)^6+1.84(10^5)\exp\{-12.00(r/r_v)\}\right]\\
U_{\mu\mu'} &= \frac{14.3928[\mu\mu'(\cos\chi-3\cos\alpha\cos\alpha')]}{R^3D}
\end{aligned}
\tag{1}
$$

Parameters r, θ, θ' and ϕ in Eq. (1) are shown in Fig. 1(a). Variables θ and θ' appearing in $U_{\theta\theta'}$ are two bond angles centered at the same atom. If an atom is bonded to three other atoms, the angle between one of the bonds and the plane defined by the three adjacent atoms is represented by γ. Variables r and r' in the expression for $U_{s\theta}$ equal lengths of the two bonds which make angle θ between them. A subscript, 0, on a variable represents its value in the configuration of the minimum potential energy with

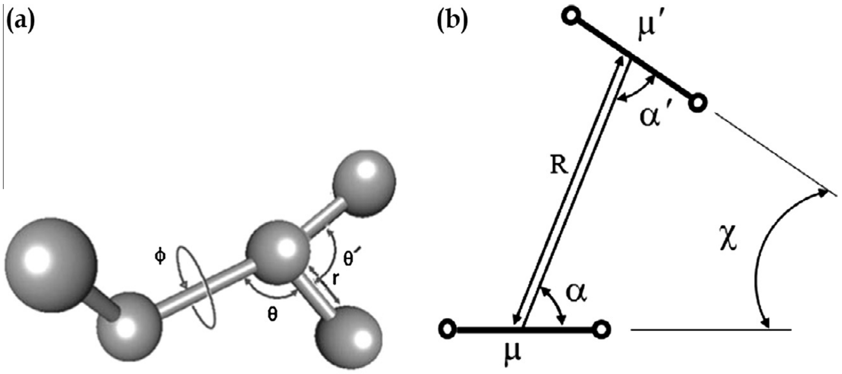

Fig. 1. Definitions of some variables in the MM3 potential. (a) Parameters r, θ, θ' and ϕ [12]; (b) parameters in dipole–dipole interaction [22].

no external loads applied to the SLGS. Material parameters ε and r_v represent an energy scale factor and the van der Waals distance, respectively. As depicted in Fig. 1(b), variables μ and μ' are bond centered dipole moments, χ is the angle between two dipoles, α and α' are angles made by two dipoles with the line connecting their centers, and R is the distance between their centers. Values of constants K_s, K_θ, K_γ, V_1, V_2, V_3, ε, r_v, $K_{s\theta}$, $K_{s\phi}$, $K_{\theta\theta'}$, and D given by Ponder [21] are used in this work.

2.2. Modeling of functionalized SLGSs

Functionalization of a finite zigzag SLGS of size 50 Å × 50 Å is considered as a model problem. The molecular structure of a functionalized SLGS is obtained from topologies of the pristine SLGS and the functional group. All simulations are done with a cut-off distance of 9.5 Å and at zero Kelvin. First, the potential energy of the SLGS is minimized by using the steepest decent algorithm with the root mean square (rms) gradient of 0.001 kcal/mol/Å to obtain its relaxed configuration. The size of the relaxed sheet is found to be 47.10 Å × 47.75 Å. The functional group is then positioned adjacent to a carbon atom of the relaxed SLGS and the potential energy of the structure is minimized to obtain the relaxed configuration of the functionalized SLGS. We note that the introduction of covalent bonds at the functionalized sites alters the hybridization of the affected carbon atoms from sp^2 to sp^3.

Five functional groups, namely, hydrogen, hydroxyl, carboxyl, amine, and fluorine are considered. We analyze deformations of SLGSs functionalized with each of these functional groups with the amount of functionalization varied from 0% to 10%. The percentage of functionalization is defined as the ratio of the number of carbon atoms to which atoms of a functional group are attached to the total number of carbon atoms in the SLGS. Thus zero percentage of functionalization represents the pristine SLGS. We also study hybrid functionalized SLGSs in which equal number of carbon atoms are functionalized with hydrogen and carboxyl groups.

The carbon atoms to which a functional group is attached are randomly selected. However, the same set of atoms, except for the fluorine group, is used for different functional groups to maintain consistency in numerical experiments. For an SLGS functionalized with fluorine, we could not bond fluorine atoms to two carbon atoms which are either bonded together (which makes distance between two F atoms, $d_{F-F} = 1.34$ Å) or are bonded to a common carbon atom (which corresponds to $d_{F-F} = 2.33$ Å). However, we could functionalize all carbon atoms of the SLGS with fluorine by having covalently bonds pointing upwards and downwards on alternate carbon atoms (see Fig. 4). Lee et al. [25], using DFT, found that when two fluorine atoms in a functionalized SLGS come closer than 2.892 Å, the relative energy of graphene-F_2 becomes very high that makes C—F bonding less favorable. However, they could obtain stable configuration of 100% fluorinated graphene which is consistent with the work of Johns and Hersam [26]. We also study SLGSs fully (100%) functionalized with hydrogen and hydroxyl groups. We could not fully functionalize SLGSs with either carboxyl or amine groups since the distance between two farthest atoms in these groups is larger than the C—C bond length in the SLGS.

Fig. 2 depicts schematics of the functional groups covalently bonded to a carbon atom of the SLGS. Unless otherwise mentioned, atoms in green, navy, olive, blue, and pink color represent carbon, hydrogen, oxygen, nitrogen, and fluorine, respectively. These configurations reveal that the covalent bond between the carbon atom and a functional group pulls the carbon atom out of the plane of the SLGS resulting in the distortion at the functionalized site. Fig. 3(a)–(f) exhibits schematics of SLGSs 2% functionalized with hydrogen, hydroxyl, carboxyl, amine, fluorine, and hybrid (hydrogen and carboxyl), respectively. In Fig. 4 we have depiced schematics of an SLGS 100% functionalized with the fluorine group; similar sketches for the SLGSs 100% functionalized with —H and —OH groups are not shown. In the 100% functionalized SLGSs alternate carbon atoms have a functional group covalently bonded to them pointing upwards and downwards. We note that the relaxed (or equilibrated) SLGSs partially functionalized with any of these five groups are not flat. However, the mid-surface of the 100% functionalized SLGS is indeed flat.

2.3. Virtual tension/compression and shear tests

Boundary conditions on SLGSs are applied on carbon atoms one row away from the ends in order to mitigate effects of unsaturated ends. In Fig. 5(a) and (b) we have shown displacements applied on carbon atoms at the right edge of the SLGS for simulating virtual tension and shear tests, respectively. The X- and the Y-coordinate axes are oriented along the zigzag and the armchair directions, respectively. In numerical tension/compression tests, carbon atoms on a row near one end of the SLGS are fixed and incremental axial displacements are applied to carbon atoms on the corresponding row near the other end as depicted in Fig. 5(a). After each displacement increment, the potential energy of the sheet is minimized and the strain energy of the deformed sheet is computed by subtracting from it the potential energy of the unstrained sheet. The strain energy density is computed by dividing the strain energy by the volume of the SLGS which is taken equal to that of the ECS of in-plane area equal to the undeformed but relaxed SLGS and thickness equal to 3.4 Å which is the interlayer separation in bulk graphite. We note that when the SLGS is functionalized, its in-plane area changes and the functionalized SLGS is not a perfect rectangle. In Table 2, we have listed the average length, a, and the

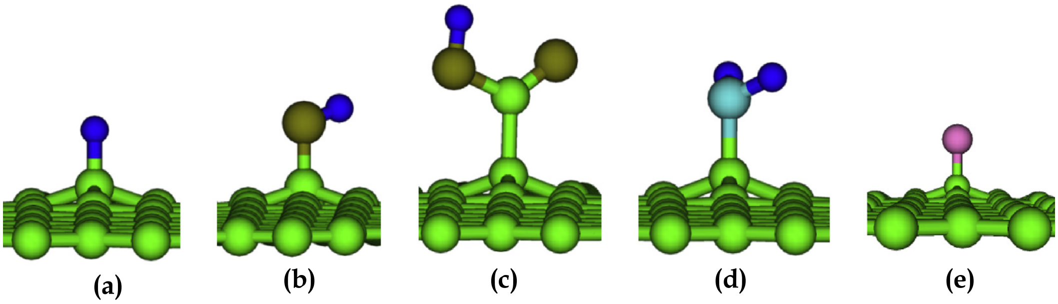

Fig. 2. Schematics of a carbon atom of the graphene attached with (a) hydrogen (—H), (b) hydroxyl (—OH), (c) carboxyl (—COOH), (d) amine (—NH_2), and (e) fluorine (—F) groups.

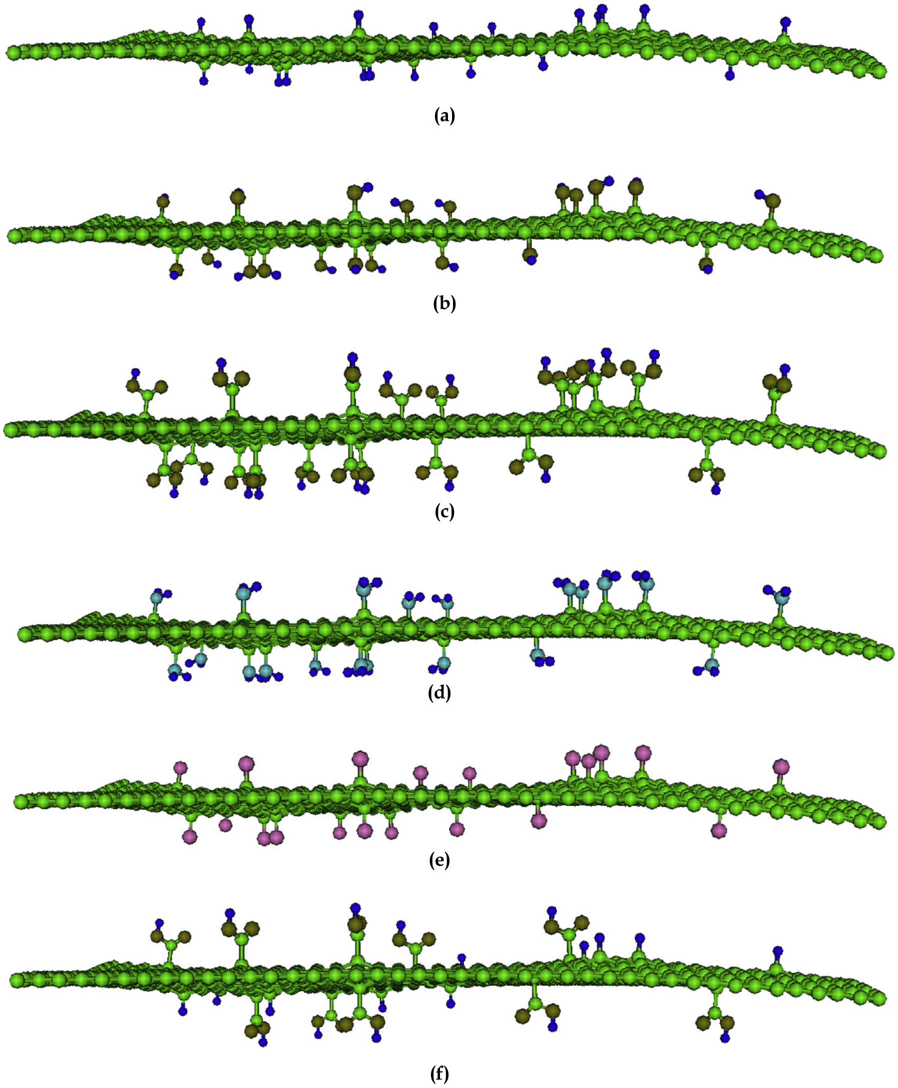

Fig. 3. Schematic sketches of SLGSs with 2% atoms functionalized with (a) —H, (b) —OH, (c) —COOH (d) —NH_2, (e) —F, and (f) hybrid groups.

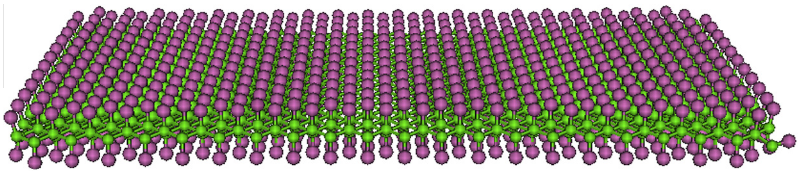

Fig. 4. Schematic sketch of an SLGS having all atoms functionalized with the —F group.

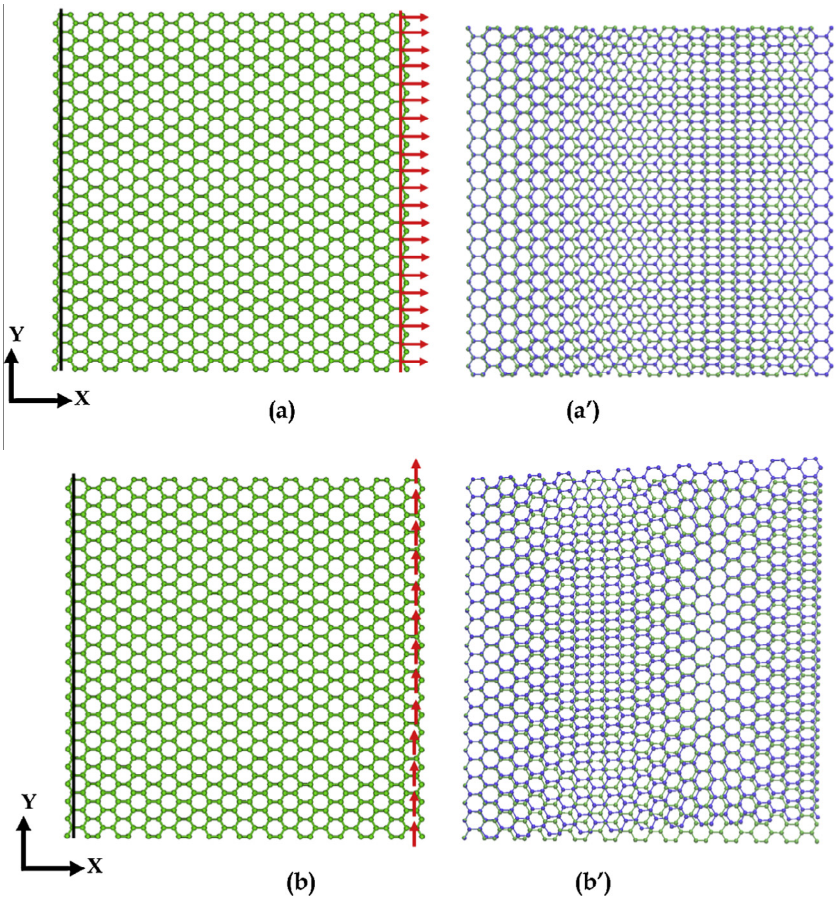

Fig. 5. For a zigzag SLGS, depiction of boundary conditions for (a) virtual tension test and (b) virtual shear test. Shapes of the SLGS deformed in tension and shear are shown in Figs. (a′) and (b′) respectively. The black line near the left edge shows the row of fixed atoms and the red line near the right edge shows the row of atoms to which displacements are applied. Structures in green and blue colors correspond to unstrained and strained SLGSs, respectively. (For interpretation of the references to color in this figure legend, the reader is referred to the web version of this article.)

Table 2
Average length and average width of functionalized SLGS in their relaxed configurations.

% Functionalization	Hydrogen		Hydroxyl		Carboxyl		Amine		Fluorine		Hybrid	
	a (Å)	*b* (Å)	*a* (Å)	*b* (Å)	*a* (Å)	*b* (Å)	*a* (Å)	*b* (Å)	*a* (Å)	*b* (Å)	*a* (Å)	*b* (Å)
2	45.89	45.56	45.88	45.55	45.86	45.54	45.86	45.53	45.86	45.54	45.88	45.55
4	46.00	45.71	45.98	45.70	45.95	45.68	45.95	45.66	45.96	45.65	45.98	45.69
6	46.08	45.82	46.05	45.80	45.99	45.73	45.99	45.73	45.99	45.79	46.04	45.79
8	46.15	45.78	46.12	45.76	46.01	45.63	46.03	45.65	46.09	45.73	46.11	45.75
10	46.12	45.65	46.04	45.59	45.93	45.37	45.95	45.43	46.06	45.69	46.08	45.72
100	49.66	48.02	51.84	50.88	–	–	–	–	49.62	49.29	–	–

average width, *b*, of each functionalized sheet which are used to calculate the in-plane area of the sheet.

A polynomial is fitted by the least squares method to the data points (strain energy density, axial strain). The first and the second derivatives of the strain energy density with respect to the axial strain yield the corresponding average axial stress and the average Young's modulus, respectively. This procedure is the same as that used by Gupta and Batra [12] and by Sears and Batra [27] to find Young's modulus of an SGLS and an SWCNT, respectively. Furthermore, when axial tensile/compressive strain is applied to the SLGS, transverse strain is developed in the sheet due to Poisson's effect. For infinitesimal deformations, the negative of the ratio of the transverse strain (away from the fixed left edge) to the axial strain equals Poisson's ratio. Similarly, the SLGSs are deformed in simple shear by applying tangential displacements rather than axial displacements as shown in Fig. 5(b) and the average shear modulus is computed as the second derivative of the strain energy of shear deformation with respect to the shear strain. The shapes of the pristine SLGS deformed in tension and shear are displayed in Fig. 5(a') and (b'), respectively.

3. Results

3.1. Validation of functionalization

In the relaxed configuration of the functionalized SLGS, the equilibrium bond length between carbon atoms of the graphene and the adjoining atoms of the functional group, if present, is computed. In Fig. 6 we have displayed a typical portion of the SLGS. When a hydrogen atom is attached to atom 1 in the Fig., the resulting bond lengths and bond angles are summarized in Table 3. We note that the torsion angle between atoms a–c–d and b–c–d is the angle between the planes defined by atoms {a, c, d} and {b, c, d} and the H—C—C is the angle H-1–3.

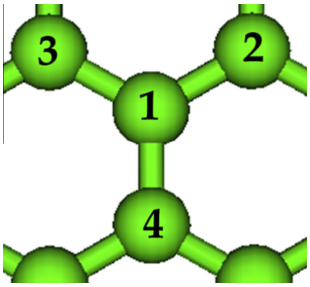

Fig. 6. A portion of the pristine SLGS.

Table 3
Values of various parameters for the pristine SLGS and a functionalized SLGS.

	Pristine SLGS	—H functionalized SLGS
Bond lengths (Å)		
1–2 Length	1.34	1.49
1–3 Length	1.35	1.49
2–3 Length	1.35	1.49
C—H Length	–	1.12
Bond angles (°)		
4–1–3 Angle	119.91	112.35
4–1–2 Angle	120	112.21
3–1–2 Angle	120	112.22
H—C—C Angle	–	106.67
Torsion angles (°)		
Angle between 4–1–3 and 2–1–3	−180	−127.42
Angle between 4–1–2 and 3–1–2	−180	127.39
Angle between 3–1–4 and 2–1–4	−180	127.37

The C—C length, 1.49 Å reported in Table 3 agrees well with 1.493 Å [28], and the C—H length, 1.12 Å listed in Table 3 compares well with 1.125 Å [28] and 1.13 Å [29] obtained with DFT calculations. Dzhurakhalov and Peeters [30] studied hydrogenation of a SLGS using the second generation reactive empirical bond order Brenner inter-atomic potential. They found C—C and C—H lengths to be 1.52 Å and 1.09 Å, respectively, and H—C—C and C—C—C angles to be 107.2° and 111.6°, respectively, which are comparable with those reported in Table 3.

The C—F bond length in the 100% fluorine functionalized SLGS at 0 K is found to be 1.37 Å, which compares well with 1.36–1.37 Å given by ab initio calculations [31] and 1.41 Å [32], and 1.40 Å [33] given by the reactive force field (ReaxFF) potential at the room temperature. Also, the C—C bond length in this fluorinated sheet at 0 K is found to be 1.51 Å compared to 1.58 Å given by ReaxFF potential [32] at room temperature.

Methanol (CH_3OH), acetic acid (CH_3COOH), and amino methane (CH_3NH_2) are simple structures representing covalent bonds between a sp^3 hybridized carbon and hydroxyl, carboxyl, and amine functional groups, respectively. These structures are generated by using the simplified molecular-input line-entry system (SMILES) [34,35] which is used to describe the structure of a chemical molecule shown in Fig. 7.

In order to validate the functionalization of the SLGS with hydroxyl, carboxyl, and amine groups, the bond angles and the bond lengths of the functional groups in the relaxed configuration of the functionalized SLGSs have been measured and compared in Tables 4–6 with those in methanol, acetic acid and amino methane. It is evident that there is good agreement between the two sets of values.

3.2. Potential energies of functionalized SLGSs

In Fig. 8 we have plotted potential energies of the functionalized SLGSs in their relaxed configuration as a function of the amount of

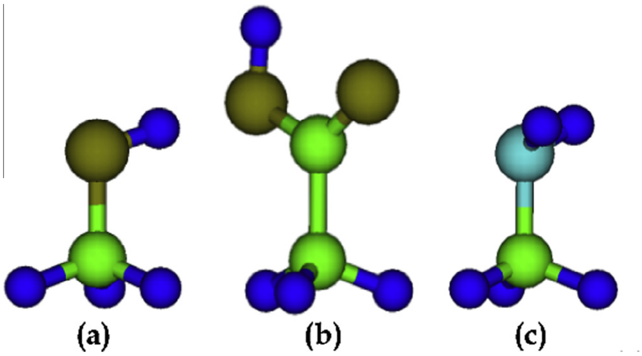

Fig. 7. Structures of (a) methanol, (b) acetic acid, and (c) amino methane generated using SMILES.

Table 4
Values of geometric parameters in the hydroxyl group.

	Methanol	—OH functionalized SLGS
R—O—H angle (°)	108.13	109.42
R—O length (Å)	1.43	1.43
O—H length (Å)	0.95	0.95

R denotes sp^3 hybridized carbon atom.

Table 5
Values of geometric parameters in the carboxyl group.

	Acetic acid	—COOH functionalized SLGS
C—O—H angle (°)	107.39	108.02
R—C—O angle (°)	112.04	112.70
R—C=O angle (°)	126.04	126.28
C—O length (Å)	1.35	1.35
C=O length (Å)	1.20	1.21
O—H length (Å)	0.97	0.97
R—C length (Å)	1.50	1.55

R denotes sp^3 hybridized carbon atom.

Table 6
Values of geometric parameters in the amine group.

	Amino methane	—NH_2 functionalized SLGS
H—N—H bond angle (°)	106.35	106.35
R—N—H bond angle (°)	112.35	113.45
Dihedral angle between two R—N—H planes (°)	119.78	121.64
N—H bond length (Å)	1.01	1.02
R—N bond length (Å)	1.46	1.46

R denotes sp^3 hybridized carbon atom.

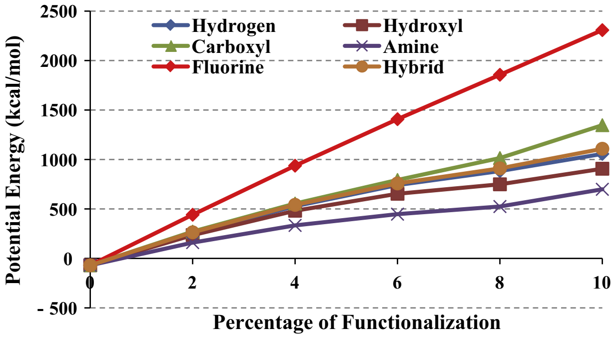

Fig. 8. Potential energies in the relaxed configuration of SLGS vs. the percentage of functionalization with (a) —H, (b) —OH, (c) —COOH, (d) —NH_2, (e) —F and (f) hybrid groups.

functionalization. These plots reveal that the potential energy of the functionalized SLGS monotonically increases with the amount of functionalization. We have shown in Fig. 9(a)–(f) the contribution from each term of the MM3 potential to the total potential energies of —H, —OH, —COOH, —NH_2, —F, and hybrid functionalized SLGSs, respectively.

Results presented in Fig. 9(a)–(f) indicate that the functionalization influences energies due to bond stretching, angle bending, torsion and van der Waals interactions. Only for the SLGS functionalized with hydroxyl, carboxyl, and amine groups, the dipole–dipole interactions contribute noticeably to the potential energy of the system. The functionalization alters bond lengths, bond angles and torsion angles as evidenced by values listed in Table 3. These increase energies due to bond stretching, angle bending and torsion energy components, as illustrated, respectively, by their values depicted in Fig. 9.

3.3. Local strains due to functionalization

The configurations depicted in Figs. 2 and 3 indicate that the functionalization deforms the SLGS by pulling the affected carbon atom out of the plane which may introduce high local strains in the SLGS at the functionalized sites. We determine these local strains by assuming that the SLGS can be regarded as a continuum structure. First we compute displacements (u, v, w) of all carbon atoms of the SLGS from their coordinates (x, y, z) in the relaxed functionalized and (X, Y, Z) in the relaxed pristine configurations from the relations

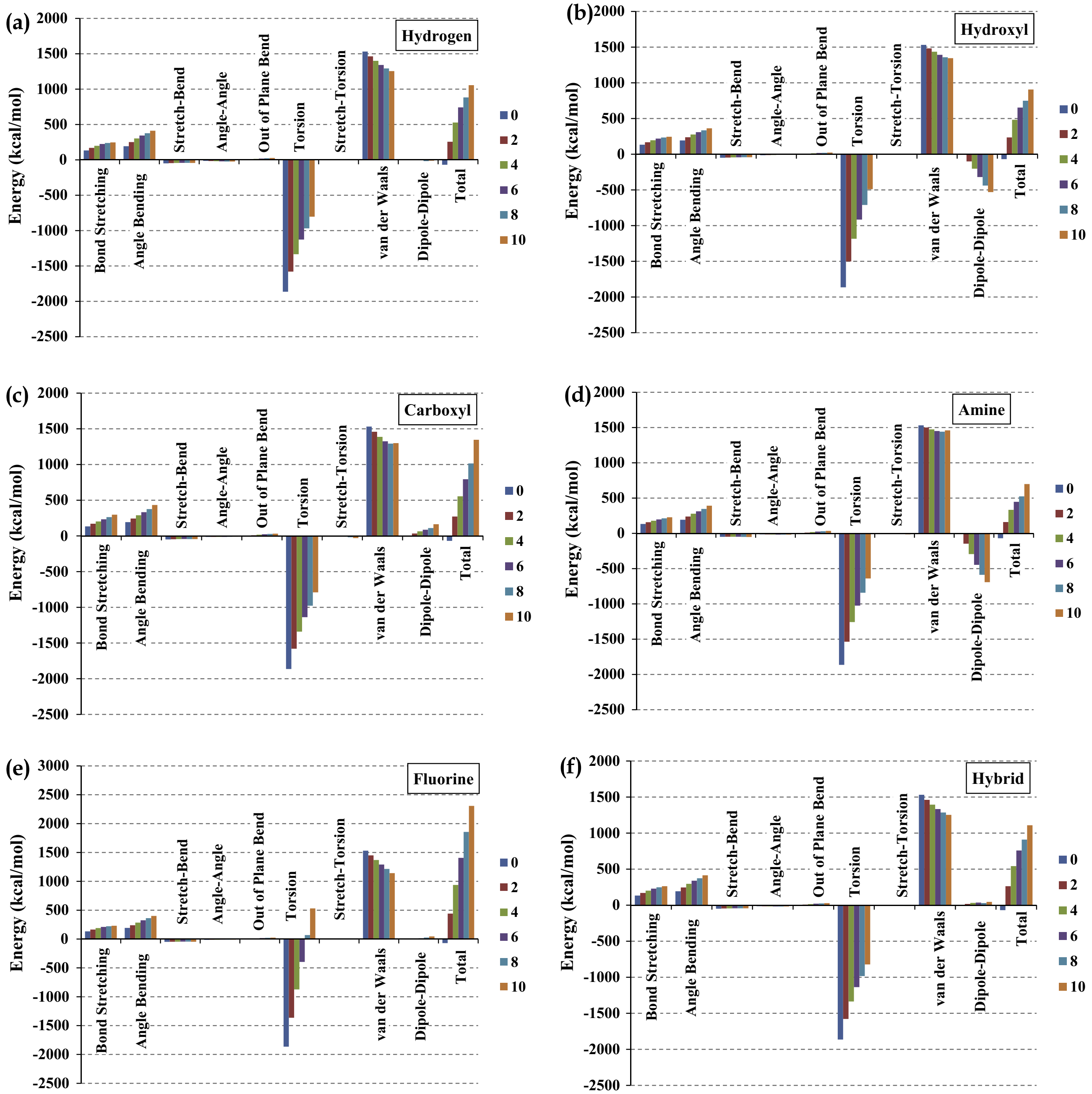

Fig. 9. For 0%, 2%, ..., 10% functionalization, individual energy components for the relaxed configurations of (a) —H, (b) —OH, (c) —COOH, (d) —NH_2, (e) —F and (f) hybrid functionalized SLGSs.

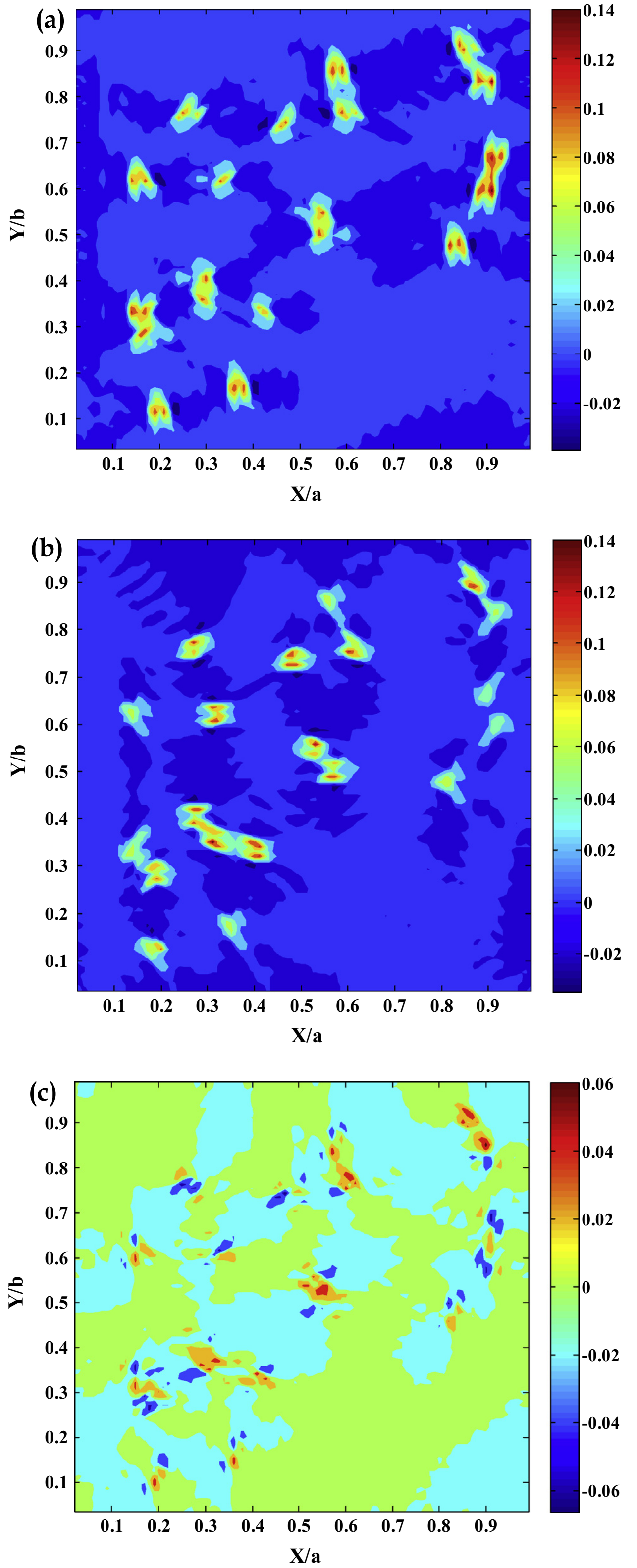

Fig. 10. Components of the Green-St. Venant strain tensor (a) E_{xx}, (b) E_{yy}, and (c) E_{xy} in the SLGS 2% functionalized with the —H group.

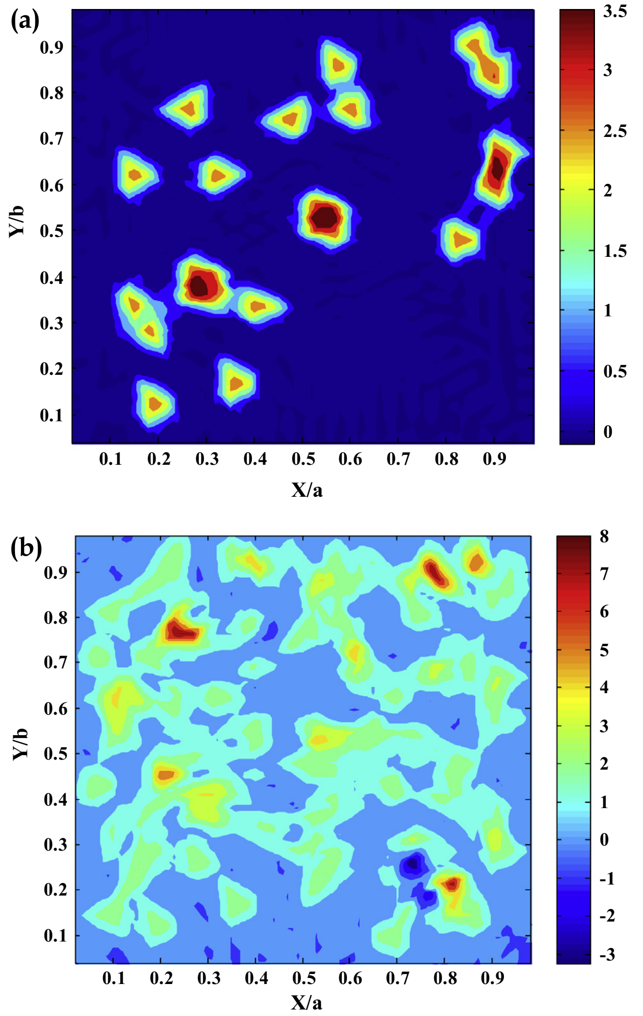

Fig. 11. Strain energy of deformation (kcal/mol) of the SLGS due to (a) 2%, and (b) 10% of —H functionalization.

$$u = x - X, \quad v = y - Y, \quad w = z - Z \tag{2}$$

Note that the relaxed pristine SLGS is flat at 0 K, hence Z-coordinates of all carbon atoms are zero. Next, we use in-built functions in MATLAB to interpolate displacements at a point in the continuum sheet and compute the displacement gradients at various points. From values of the displacement gradients, we find in-plane components of the Green-St. Venant strain tensor, **E**, from the following equations [36]:

$$E_{ij} = \frac{1}{2}\left[\frac{\partial u_i}{\partial X_j} + \frac{\partial u_j}{\partial X_i} + \frac{\partial u_k}{\partial X_i}\frac{\partial u_k}{\partial X_j}\right] \quad (i, j = 1, 2;\ k = 1, 2, 3) \tag{3}$$

Unless mentioned otherwise, (u_1, u_2, u_3) represent (u, v, w). In Eq. (3), (X_1, X_2) correspond to (X, Y) and E_{11}, E_{22}, E_{12} represent E_{xx}, E_{yy}, E_{xy}, respectively. Furthermore, the repeated index k implies summation over its range, 1, 2, and 3. In Fig. 10 we have exhibited fringe plots of E_{xx}, E_{yy} and E_{xy} in the SLGS 2% functionalized with —H group; that for the —OH group is similar to the one for the —H group. The coordinate axes have been normalized with their lengths a = 47.10 Å and b = 47.75 Å in the relaxed configuration of the pristine SLGS. These plots suggest that the magnitude of the local axial strain, E_{xx} or E_{yy}, at the functionalized sites of both sheets is about 0.14 even when the potential energy of the functionalized SLGS has been minimized. The maximum in-plane shear strain, E_{xy}, equals about 0.06. Similar results are obtained for the SLGS functionalized with other functional groups but are omitted for the sake of the brevity. We note that since the plane of the SLGS is defined by Z = 0, we cannot obtain transverse components of the Green-St. Venant strain tensor, **E**. However, we can

Table 7
Maximum values of components of the Almansi–Hamel strain tensor in SLGS 2% functionalized with —H and —OH groups.

Maximum values of strain components	—H	—OH
η_{xx}	0.10	0.09
η_{yy}	0.10	0.09
η_{zz}	1.28	1.16
η_{xy}	0.05	0.06
η_{xz}	0.93	0.90
η_{yz}	0.56	0.79
η_{e}	2.28	2.15

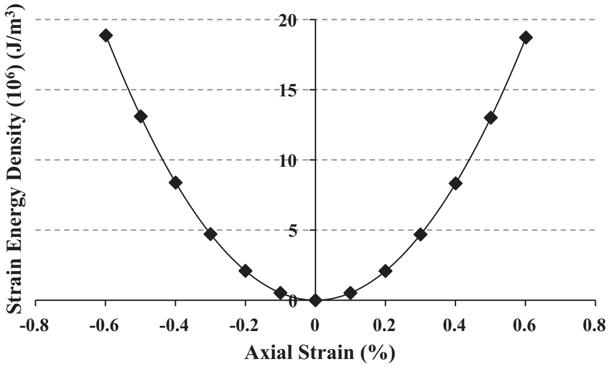

Fig. 12. Strain energy density of the pristine SLGS vs. the axial strain computed using the MM3 potential.

obtain all six components of the Almansi–Hamel strain tensor, η, from the following equations since the z-coordinates of carbon atoms are nonzero in the functionalized or the current configuration [36].

$$\eta_{ij} = \frac{1}{2}\left[\frac{\partial u_i}{\partial x_j} + \frac{\partial u_j}{\partial x_i} - \frac{\partial u_k}{\partial x_i}\frac{\partial u_k}{\partial x_j}\right] \quad (i,\ j,\ k = 1, 2, 3) \tag{4}$$

In Eq. (4), (x_1, x_2, x_3) correspond to (x, y, z) and η_{11}, η_{22}, η_{33}, η_{12}, η_{13}, η_{23} represent η_{xx}, η_{yy}, η_{zz}, η_{xy}, η_{xz}, η_{yz}, respectively.

The maximum values of components of the Almansi–Hamel strain tensor in 2% —H and —OH functionalized SLGSs, listed in Table 7, indicate that functionalization can induce very high (~120%) values of the transverse normal and the transverse shear strains. We note that of all six components of Almansi–Hamel strain tensor at a point, transverse normal strain is dominant. From the components of Almansi–Hamel strain tensor, we calculate the effective strain, η_e [36] using Eq. (5). The values of the effective strain in 2% —H and —OH functionalized sheets as reported in Table 7 are found to be more than 200%.

$$\eta_e = \sqrt{\frac{3}{2}\left(\eta_{xx}^2 + \eta_{yy}^2 + \eta_{zz}^2 + 2\eta_{xy}^2 + 2\eta_{xz}^2 + 2\eta_{yz}^2\right)} \tag{5}$$

The sheets may rupture during the functionalization process due to such high local strains induced in them. However, no failure criteria are included in our work.

For elastic deformations stresses at a point are unique functions of strains at that point. Thus stresses at points of high strains will also have high values. Namilae et al. [37] computed stresses at the sites of functionalized atoms in their molecular dynamics simulations of functionalized SWCNTs. We note that the computation of stresses usually (e.g. by the Hardy method [38]) requires averaging over a small domain that can smear out their values. Hardy's method requires averaging over a sphere centered at the point of interest in the current configuration, and thus cannot be easily adapted to the current situation because of the scarcity of atoms in the sphere with the center at the functionalized carbon atom.

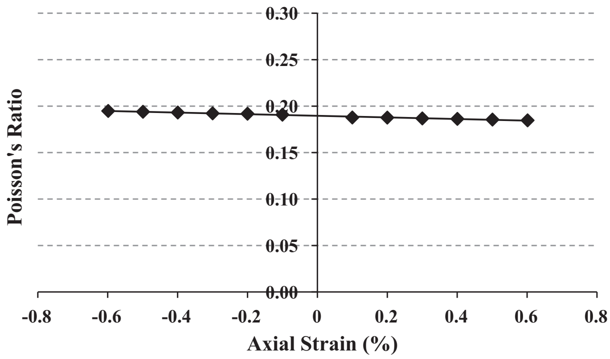

Fig. 13. Poisson's ratio vs. axial strain for the pristine SLGS.

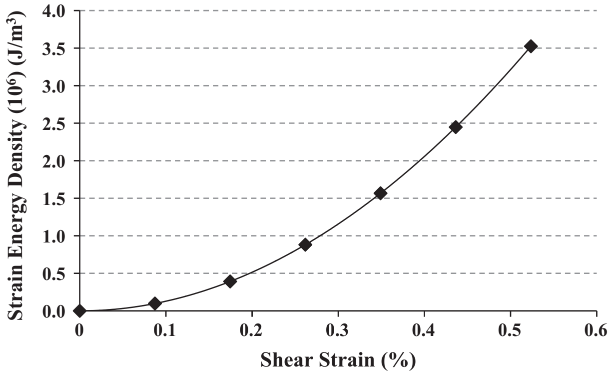

Fig. 14. Strain energy density of the pristine SLGS vs. the shear strain computed using the MM3 potential.

Another measure of deformations of the SLGS due to functionalization is the strain energy of deformation. In Fig. 11(a) and (b) we have depicted fringe plots of the strain energy of the SLGS in kcal/mol due to 2% and 10% of hydrogen functionalization, respectively. We note that the scales used in the two Figures are different. The maximum strain energy in the 10% hydrogen functionalized SLGS is about twice of that in the 2% hydrogen functionalized SLGS.

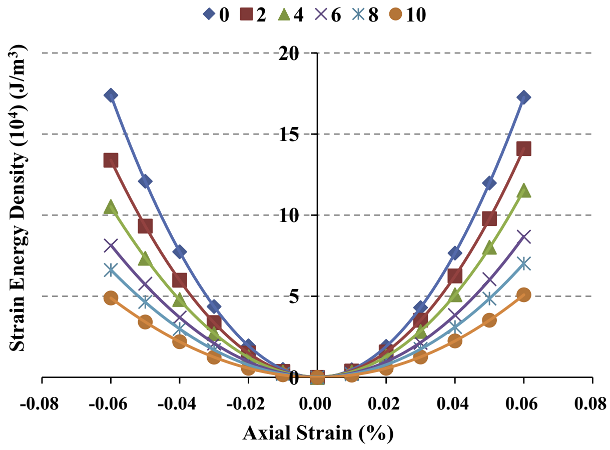

Fig. 15. Variation of the strain energy density with the axial strain for the —COOH functionalized SLGSs with the percentage of functionalization varied from 0% to 10%.

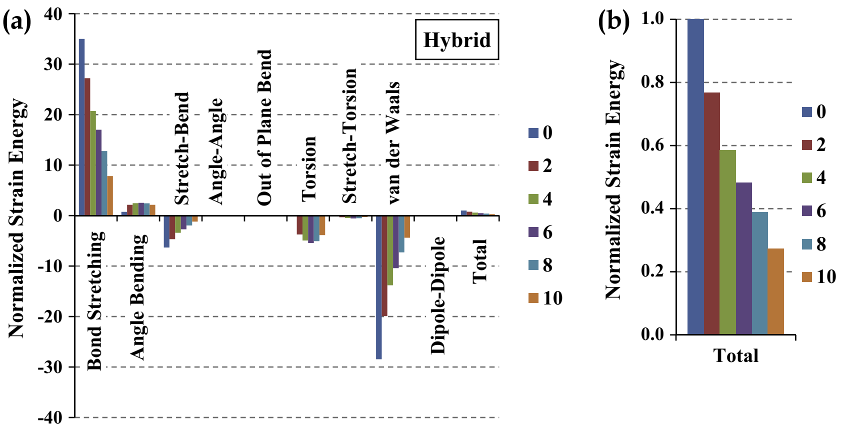

Fig. 16. (a) Break down of the total strain energy of deformation (at 0.06% tensile strain) into individual energy components for hybrid functionalized SLGSs with percentage of functionalization varying from 0% to 10%, and (b) the total strain energy on magnified scale.

Table 8
Young's modulus of the SLGSs functionalized with different groups.

Young's Modulus (TPa)						
% Functionalization	Hydrogen	Hydroxyl	Carboxyl	Amine	Fluorine	Hybrid
0	1.04	1.04	1.04	1.04	1.04	1.04
2	0.78	0.76	0.76	0.78	0.76	0.77
4	0.54	0.53	0.61	0.61	0.47	0.59
6	0.44	0.44	0.47	0.49	0.37	0.47
8	0.37	0.36	0.38	0.41	0.32	0.39
10	0.28	0.25	0.28	0.28	0.22	0.28
100	0.54	0.72	–	–	0.52	–

3.4. Results of virtual experiments

The pristine and functionalized zigzag SLGSs are deformed in tension/compression and shear and values of the elastic moduli are deduced by the method described in Section 2.3.

3.4.1. Pristine SLGS

The variation of the computed strain energy density with the axial strain for the pristine SLGS is shown in Fig. 12.

The third order polynomial fit to the data with the regression coefficient of 1.0 is

$$W_v = -7.53(10^{11})\in^3 + 5.22(10^{11})\in^2 - 1.04(10^6)\in \tag{6}$$

where W_v is the strain energy density in J/m^3 and $\in$ is the nominal axial strain. Thus, expressions for the axial stress σ and the modulus of elasticity, E, in Pa are

$$\sigma = -2.26(10^{12})\in^2 + 1.04(10^{12})\in - 1.04(10^6) \tag{7}$$

$$E = -4.52(10^{12})\in + 1.04(10^{12}) \tag{8}$$

Young's modulus, E, at zero strain is 1.04 TPa which corresponds to the basal plane stiffness, K, of 353.6 N/m. This value of E or K compares well with the range of values reported in Table 1 obtained using various methods. Eq. (8) indicates that E for an axially stretched SLGS decreases with an increase in the axial strain. Furthermore, for the same value of the axial strain, E is lower for the axially stretched sheet than that of an axially compressed SLGS. Furthermore, from results of the tension/compression tests, the computed variation of Poisson's ratio (or function) with the axial strain plotted in Fig. 13 shows that Poisson's ratio at zero strain equals 0.19. This value of Poisson's

Table 9
Basal plane stiffness (K) of fully functionalized SLGS with —H and —F reported by various investigators.

Reference	Method/potential	Functional group	K (N/m)
Present	MM/MM3	—H	183.6
		—F	176.8
Pei et al. [17]	MD/AIREBO	—H	200.6
Li et al. [41]	MD/AIREBO	—H	204.0
Leenaerts et al. [42]	DFT	—H	241.4
		—F	224.4
Cadelano and Colombo [43]	Combined continuum elasticity and DFT	—H	217.6
Singh et al. [32]	MD/ReaxFF	—F	250.0

Table 10
Shear modulus of the SLGSs functionalized with different groups.

Shear Modulus (TPa)						
% Functionalization	Hydrogen	Hydroxyl	Carboxyl	Amine	Fluorine	Hybrid
0	0.26	0.26	0.26	0.26	0.26	0.26
2	0.21	0.21	0.21	0.21	0.21	0.21
4	0.18	0.18	0.17	0.17	0.16	0.18
6	0.14	0.14	0.14	0.14	0.11	0.14
8	0.15	0.15	0.14	0.15	0.14	0.15
10	0.15	0.14	0.14	0.15	0.13	0.15
100	0.16	0.15	–	–	0.17	–

ratio agrees well with 0.186 given by ab initio calculations [2], 0.18 given by DFT calculations [6] and 0.21 given by MM simulations [12]. Poisson's ratio slowly decreases with an increase in the axial strain.

In Fig. 14 we have illustrated the strain energy density vs. the shear strain for the pristine SLGS. The third order polynomial fitted through data points with the regression coefficient of 1.0 is

$$W_v = -4.67(10^9)\gamma^3 + 1.29(10^{11})\gamma^2 - 4.17(10^4)\gamma \qquad (9)$$

where γ is the shear strain. Thus, expressions for the shear stress τ and the shear modulus G in Pa are

$$\tau = -1.40(10^{10})\gamma^2 + 2.58(10^{11})\gamma - 4.17(10^4) \qquad (10)$$

$$G = -2.80(10^{10})\gamma + 2.58(10^{11}) \qquad (11)$$

The shear modulus at zero shear strain equals 0.26 TPa which agrees with 0.28 TPa [39] found experimentally, 0.28 TPa [19] and 0.29 TPa [20] computed by MD simulations, and 0.22 TPa obtained by atomistic simulations [40].

Table 11
Average values of *E* and *G* for five groups of randomly selected carbon atoms for 4% —H functionalized SLGS.

Sample	*E* (TPa)	*G* (TPa)
1	0.54	0.18
2	0.62	0.22
3	0.56	0.22
4	0.64	0.21
5	0.63	0.19
% Standard deviation	4.07	1.59

Table 12
Values of *E* and *G* for pristine and 4% functionalized zigzag and armchair SLGSs.

SLGS	*E* (TPa)			*G* (TPa)		
	Zigzag	Armchair	% Difference	Zigzag	Armchair	% Difference
Pristine	1.04	1.04	0	0.26	0.26	0
—H	0.54	0.38	28	0.18	0.22	−18
—OH	0.53	0.38	27	0.18	0.22	−22
—COOH	0.61	0.46	25	0.17	0.22	−24
—NH_2	0.61	0.46	25	0.17	0.13	−27
—F	0.47	0.38	19	0.16	0.21	−29

Table 13
Values of *E* and *G* for pristine and 4% functionalized zigzag SLGSs of different sizes.

Unrelaxed size	*E* (TPa)		*G* (TPa)	
	Pristine	4% —H functionalized	Pristine	4% —H functionalized
50 Å × 50 Å	1.04	0.54	0.26	0.18
75 Å × 75 Å	1.03	0.48	0.27	0.16
100 Å × 100 Å	1.02	0.46	0.26	0.11
Standard deviation	0.01	0.04	0.006	0.036

3.4.2. Functionalized SLGSs

3.4.2.1. Young's modulus. For hydrogen, hydroxyl, carboxyl, amine, fluorine, and hybrid functionalized SLGSs, the strain energy density vs. the axial strain curves for different percentages of functionalization were plotted. Since they are similar for each functional group, only those for the carboxyl group are depicted in Fig. 15. The applied compressive axial strains are kept small enough to avoid local bucking due to non-uniformities in the structure of the functionalized SLGSs. Results in these plots evince that for each value of the axial strain the functionalization reduces the strain energy of deformation from that of the pristine SLGS. In order to better understand the effect of functionalization on the strain energy of deformation, we have exhibited in Fig. 16 the contribution of different energy terms to the total strain energy of deformation at 0.06% axial strain due to the six functionalization groups studied.

The normalized strain energies plotted in Fig. 16 reveal that the functionalization mainly reduces the strain energy associated with the bond stretching component of the MM3 potential and increases the strain energy due to van der Waals interaction. However, as a net effect, the total strain energy of the SLGS decreases due to functionalization and the reduction in the strain energy increases with an increase in the percentage of functionalization. We note that energie: in Fig. 16 are normalized with respect to the strain energy of the pristine SLG: at 0.06% axial strain.

The axial stress–axial strain curves for the —NH_2 functionalized SLGS deformed in simple tension are plotted in Fig. 17; curves for the other functional groups are omitted since they are similar to those shown for the —NH_2 group.

These results suggest that the functionalization reduces the slope of the axial stress–axial strain curve and hence Young's modulus, *E*, of the functionalized sheet is less than that of the pristine sheet. Moreover the value of *E* decreases with an increase in the percentage of functionalization. This reduction in the value of *E* could be caused by the local high strains induced in the SLGS due to functionalization as evidenced by results exhibited in

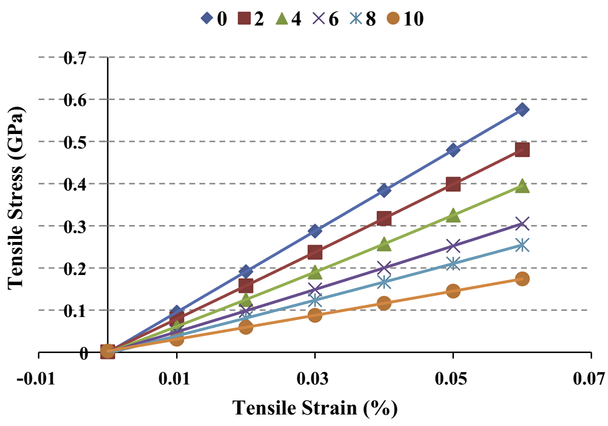

Fig. 17. For 0–10% functionalization, the axial stress–axial strain curves for the —NH_2 functionalized SLGSs deformed in tension.

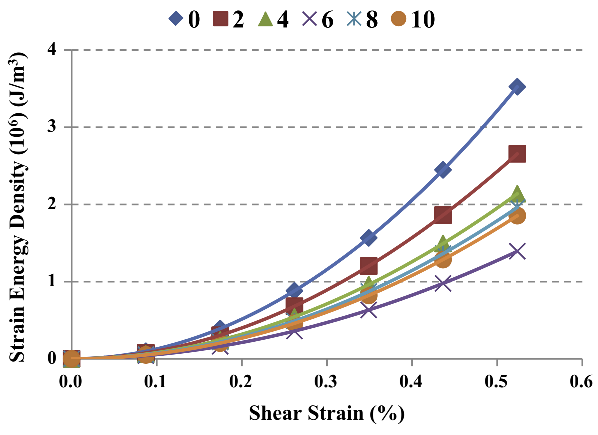

Fig. 18. Variation of the strain energy density with the shear strain for the —F functionalized SLGSs with the percentage of functionalization varied from 0% to 10%.

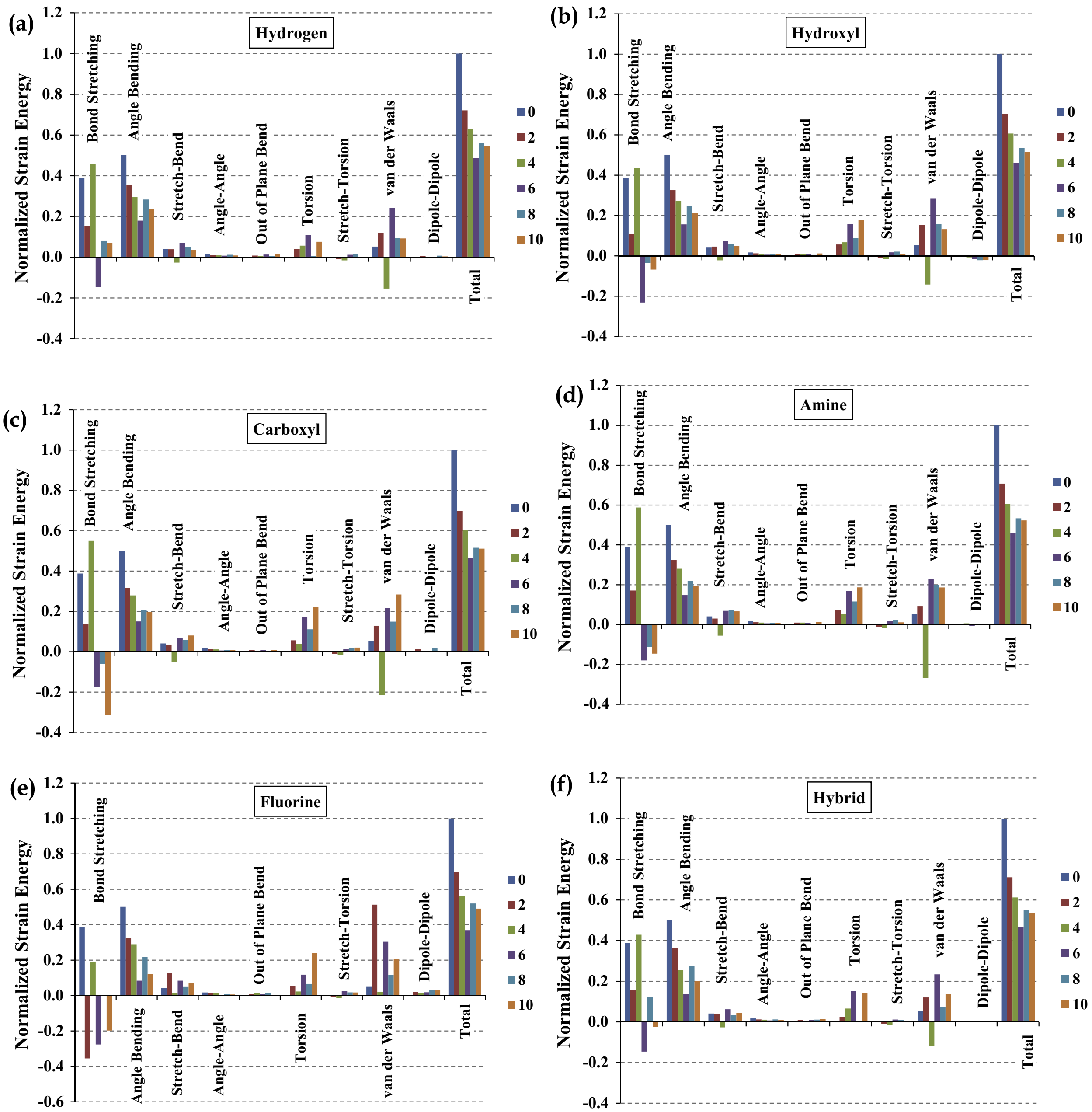

Fig. 19. Break down of the total strain energy of deformation (at 0.52% shear strain) into individual energy components for (a) —H, (b) —OH, (c) —COOH, (d) —NH_2, (e) —F, and (f) hybrid functionalized SLGSs with percentage of functionalization varying from 0% to 10%.

Figs. 10 and 11. Values of *E* for the functionalized SLGSs for different percentages of functionalization are listed in Table 8. These values are found by using average values of the axial strain and the axial stress.

Values of *E* listed in Table 8 suggest that *E* decreases with an increase in the amount of functionalization, is nearly independent of the functionalizing agent, and *E* for fully functionalized SLGS is about the same as that for the 2–4% functionalized SLGS. The relaxed configuration of the unloaded fully functionalized SLGS is flat and there are no high local strains induced in it. Thus deformations of the fully functionalized SLGS are nearly homogeneous but those of the partially functionalized SLGS are inhomogeneous. The values of the basal plane stiffness *K* of fully functionalized SLGSs displayed in Table 9 shows that our results agree with those obtained by other investigators.

In order to check if any inelastic deformations had been introduced during the numerical experiments, we unloaded the SLGS and found for a given value of the axial displacement, the strain energy of deformation during loading equaled that during unloading.

3.4.2.2. Shear modulus. We have plotted in Fig. 18 the strain energy density vs. the shear strain curves for the fluorine functionalized SLGS which are typical for the six functional groups studied. These results suggest that the functionalization reduces the strain energy of shear deformation from that of the pristine SLGS, and the reduction in the strain energy increases with an increase in the amount of functionalization. However, the strain energy does not vary much with the increase in the amount of functionalization beyond 6%. Furthermore, the decrease in the strain energy density is not monotone with respect to the increase in the amount of functionalization.

The contribution from different components to the total strain energy of shear deformation for the SLGSs functionalized with —H, —OH, —COOH, —NH_2, —F, and hybrid groups are depicted in Fig. 19(a)–(f), respectively. Note that the energies depicted in Fig. 19 are normalized with respect to the strain energy of shear deformation of the pristine SLGS. These results suggest that while various components affect the strain energy, the net effect is a decrease in the strain energy of the SLGS when it is functionalized.

In Table 10 we have listed values of the shear modulus of the SLGS functionalized with different functional groups and for varying percentage of functionalization.

Values reported in Table 10 suggest that the functionalization decreases the shear modulus of the SLGS, and the reduction is essentially the same for different functional groups. The shear modulus is found to decrease monotonically with an increase in the percentage of functionalization up to 6%, beyond that it does not change much. The value 0.15 TPa of the shear modulus for 8% —OH functionalized SLGS compares well with 0.17 TPa [19] obtained using MD simulation with the COMPASS force field for 7.5% —OH functionalization.

In our study of SWCNTs [22], we found 61% and 55% reduction in the values of E and G, respectively, when the SWCNT is 100% functionalized with the hydrogen group. Here E and G for the SLGS are found to decrease by 48% and 38%, respectively, suggesting that a fully functionalized SLGS may be a better candidate for reinforcement in nano-composites than a fully functionalized SWCNT. Of course, the two reinforcements have different shapes and will provide strengths in different directions of the composite.

3.4.3. Effect of random selection of atoms on values of elastic moduli

As stated before the carbon atoms for functionalization are randomly selected. For the SLGS functionalized with the —H group, we conducted numerical experiments in tension/compression and shear for five sets of 4% randomly selected carbon atoms to which functional groups were attached. The average values of E and G listed in Table 11 differ from each other by 4% and 1.6%, respectively, implying that the selection of carbon atoms for functionalization has virtually no effect on the mean value of the elastic moduli of functionalized SLGSs.

3.4.4. Effect of chirality

In order to investigate the effect of chirality on the elastic moduli of SLGSs, we performed virtual experiments on the pristine and 4% functionalized SLGSs. In Table 12 we have listed values of the elastic moduli in the zigzag and the armchair configurations of the SLGS. With values taken in the zigzag direction as the reference values, we have computed the deviation of values in the armchair configuration. The 20–30% difference in the two values of the elastic moduli suggests that the ECS of the functionalized SLGS is not isotropic even for deformations in the plane of the sheet but that of the pristine SLGS is. Thus functionalization introduces anisotropy in the plane of the SLGS.

3.4.5. Effect of sample size of finite SLGSs

As mentioned earlier, we study deformations of a finite size sample of the SLGS. All results reported so far are for a SLGS of unrelaxed size 50 Å × 50 Å. In order to investigate the effect of sample size of an SLGS on its elastic moduli, we study deformations of two more finite SLGSs of dimensions 75 Å × 75 Å and 100 Å × 100 Å in their unrelaxed configurations. Upon relaxation, their dimensions are found to be 71.30 Å × 71.07 Å and 95.62 Å × 94.33 Å, respectively. In Table 13, we have summarized values of elastic moduli for the pristine and a 4% —H functionalized SLGS for each of three finite size samples. These values imply that the size of the finite SLGS has no major effect on the elastic moduli.

4. Conclusions

The effect of covalent functionalization on average values of Young's modulus and the shear modulus of a single layer graphene sheet (SLGS) has been studied using molecular mechanics simulations and the MM3 potential. It is found that large (~120%) local strains are induced at the sites of atoms to which functional groups are covalently bonded in a partially functionalized SLGS. Using average values of the axial strain and the axial stress, it is found that values of the two moduli decrease with an increase in the number of carbon atoms to which functional groups are attached, and this reduction in the value of the elastic moduli is the same for each one of the five functional groups studied. Approximately 73% and 42% reduction, respectively, in values of Young's and the shear moduli of the pristine SLGS occurs for 10% of functionalization. However, for a fully functionalized SLGS, values of the two elastic moduli are essentially the same as those for the SLGS with about 4% of atoms functionalized, and the reductions in the values of the two moduli are about 40%. We note that full functionalization can be achieved with only —F, —H and —OH groups. Even though the pristine SLGS behaves as an isotropic material in the plane of the SLGS, a partially functionalized SLGS behaves as an anisotropic material.

References

[1] G. van Lier, C. Van Alsenoy, V. van Doren, P. Geerlings, Chem. Phys. Lett. 326 (2000) 181–185.
[2] F. Liu, P. Ming, J. Li, Phys. Rev. B 76 (2007) 064120-1–064120-7.
[3] K.N. Kudin, G.E. Scuseria, B.I. Yakobson, Phys. Rev. B 64 (2001) 235406-01–235406-10.
[4] M. Arroyo, T. Belytschkho, Phys. Rev. B 69 (2004) 115415-01–115415-11.
[5] E. Konstantinova, S.O. Dantas, P.M.V.B. Barone, Phys. Rev. B 74 (2006) 035417-1–035417-6.
[6] R. Faccio, P. Denis, H. Pardo, C. Goyenola, A.W. Mombru, J. Phys.: Condens. Matter 21 (2009) 285304-1–285304-7.
[7] M. Klintenberg, S. Lebegue, C. Ortiz, B. Sanyal, J. Fransson, O.J. Eriksson, Phys.: Condens. Matter 21 (2009) 335502-1–335502-7.
[8] C. Lee, X. Wei, J.W. Kysar, J. Hone, Science 321 (2008) 385–388.
[9] C.D. Reddy, S. Rajendran, K.M. Liew, Nanotechnology 17 (2006) 864–870.
[10] E. Cadelano, P.L. Palla, S. Giordano, L. Colombo, Phys. Rev. Lett. 102 (2009) 235502-1–235502-4.
[11] J. Jiang, J. Wang, B. Li, Phys. Rev. B 80 (2009) 113405-1–113405-4.
[12] S.S. Gupta, R.C. Batra, J. Comput. Theor. Nanos. 7 (2010) 1–14.
[13] M. Neek-Amal, F.M. Peeters, Phys. Rev. B 82 (2010) 085432-1–085432-6.
[14] M. Neek-Amal, F.M. Peeters, J. Phys.: Condens. Matter 23 (2011) 045002-1–045002-8.
[15] A. Lajevardipour, M. Neek-Amal, F.M. Peeters, J. Phys.: Condens. Matter 24 (2012) 175303-1–175303-8.
[16] J.S. Bunch, S.S. Verbridge, J.S. Alden, A.M. van der Zande, J.M. Parpia, H.G. Craighead, P.L. McEuen, Nano Lett. 8 (2008) 2458–2462.
[17] Q.X. Pei, Y.W. Zhang, V.B. Shenoy, Carbon 48 (2010) 898–904.
[18] Q.X. Pei, Y.W. Zhang, V.B. Shenoy, Nanotechnology 21 (2010) 115709-1–115709-8.
[19] Q. Zheng, Z. Li, Y. Geng, S. Wang, J.K. Kim, J. Nanosci. Nanotechnol. 10 (2010) 1–5.
[20] A.H. Kheirkhah, E.S. Iranizad, M. Raeisi, A. Rajabpour, Solid State Commun. 177 (2014) 98–102.
[21] J.W. Ponder, Computer Code: Tinker Molecular Modeling Package, Washington University in St. Loius, St. Louis, 2000.
[22] P.H. Shah, R.C. Batra, Comp. Mater. Sci. 83 (2014) 349–361.
[23] N.L. Allinger, Y.H. Yuh, J.H. Lii, J. Am. Chem. Soc. 111 (1989) 8551–8566. and subsequent papers.
[24] N.L. Rangel, J.M. Seminario, J. Chem. Phys. 132 (2010) 125102-1–125102-4.
[25] S.S. Lee, S.W. Jang, K. Park, E.C. Jang, J.Y. Kim, D. Neuhauser, S. Lee, J. Phys. Chem. C 117 (2013) 5407–5415.
[26] J.E. Johns, M.C. Hersam, Acc. Chem. Res. 46 (2013) 77–86.
[27] A. Sears, R.C. Batra, Phys. Rev. B 69 (2004) 2354061-01–2354061-10.
[28] Z. Ao, S. Li, Graphene Simulation (2011) 54–74.
[29] Y. Miura, H. Kasai, W. Dino, H. Nakanishi, T. Sugimoto, J. Appl. Phys. 93 (2003) 3395–3400.
[30] A.A. Dzhurakhalov, F.M. Peeters, Carbon 49 (2011) 3258–3266.
[31] F. Karlicky, M. Otyepka, J. Chem. Theory Comput. 9 (2013) 4155–4164.

[32] S.K. Singh, S.G. Srinivasan, M. Neek-Amal, S. Costamagna, A.C.T. van Duin, F.M. Peeters, Phys. Rev. B 87 (2013) 104114-1–104114-6.
[33] R. Paupitz, P.A.S. Autreto, S.B. Legoas, S.G. Srinivasan, A.C.T. van Duin, D.S. Galvao, Nanotechnology 24 (2013) 035706-1–035706-8.
[34] D. Weininger, J. Chem. Inf. Comput. Sci. 28 (1988) 31–36.
[35] D. Weininger, A. Weininger, J.L. Weininger, J. Am. Chem. Soc. 29 (1989) 97–101.
[36] R.C. Batra, Elements of Continuum Mechanics, AIAA Educational Series, Vienna, 2006.
[37] S. Namilae, N. Chandra, C. Shet, Chem. Phys. Lett. 387 (2004) 247–252.
[38] R.J. Hardy, J. Chem. Phys. 76 (1982) 622–628.
[39] X. Liu, T.H. Metcalf, J.T. Robinson, B.H. Houston, F. Scarpa, Nano Lett. 12 (2012) 1013–1017.
[40] A. Sakhaee-Pour, Solid State Commun. 149 (2009) 91–95.
[41] Y. Li, D. Datta, Z. Li, V.B. Shenoy, Comput. Mater. Sci. 83 (2014) 212–216.
[42] O. Leenaerts, H. Peelaers, A.D. Hernandez-Nieves, B. Partoens, F.M. Peeters, Phys. Rev. B 82 (2010) 195436-1–195436-6.
[43] E. Cadelano, L. Colombo, Phys. Rev. B 85 (2012) 245434-1–245434-3.